

This is the post-print version of a paper published in Journal of Chromatography A

Citation for the original published paper (version of record):

A model free method for estimation of complicated adsorption isotherms in liquid chromatography. P. Forssén, T. Fornstedt. J. Chromatogr. A 1409 (2015) 108-115.

Access to the published version may require subscription.

N.B. When citing this work, cite the original published paper.

**Attribution-NonCommercial-
NoDerivatives 4.0
International**



1 A Model Free Method for Estimation of Complicated 2 Adsorption Isotherms in Liquid Chromatography

3 Patrik Forssén, Torgny Fornstedt*

4 Department of Engineering and Chemical Sciences, INTERACT, Karlstad University, SE-651 88
5 Karlstad, Sweden

6 * Corresponding author information:

7 Torgny Fornstedt, Professor, Karlstad University, SE-651 88 Karlstad, Sweden

8 Torgny.Fornstedt@kau.se, +46 76 774 31 58

9 Keywords: Adsorption isotherm, Inverse Method, Interpolation, Inflection points, Finite Volumes,
10 Equilibrium Dispersive model

11 **Abstract**

12 Here we show that even extremely small variations in the adsorption isotherm can have a
13 tremendous effect on the shape of the overloaded elution profiles and that the earlier in the
14 adsorption isotherms the variation take place, the larger its impact on the shape of the elution
15 profile. These variations are so small so that they can be “hidden” by the discretization and in the
16 general experimental noise when using traditional experimental methods, such as frontal analysis, to
17 measure adsorption isotherms. But as the effects of these variations are more clearly visible in the
18 elution profiles the Inverse Method (IM) of adsorption isotherm estimation is an option. However, IM
19 usually requires that one selects an adsorption isotherm model prior to the estimation process. Here
20 we show that even complicated models might not be able to estimate the adsorption isotherms with
21 multiple inflection points that small variations might give rise to. We therefore developed a modified
22 IM that, instead of fixed adsorption isotherm models, uses monotone piecewise interpolation. We
23 first validated the method with synthetic data and showed that it can be used to estimate an
24 adsorption isotherm which accurately predicts an extremely “strange” elution profile. For this case it
25 was impossible to estimate the adsorption isotherm using IM with a fixed adsorption model. Finally,
26 we will give an example of a real chromatographic system where adsorption isotherm with inflection
27 points is estimated by the modified IM.

28 **1 Introduction**

29 Today chromatography is increasingly important for analysis and purifications of pharmaceuticals,
30 and other valuable chemicals such as antioxidants and intermediates, both in industry and in
31 academia. However, improved technical and numerical methods for obtaining detailed knowledge
32 about the thermodynamics and mass transfer kinetics of the processes are necessary. Estimation of
33 adsorption isotherms are crucial for computer-assisted optimizations of preparative systems [1–3]
34 and also give deeper understanding of the separation processes and its molecular interactions [4,5].
35 Chiral preparative chromatography stationary phases are much more expensive than achiral ones
36 and also have more limited capacities. Therefore in this case it is especially important to accurately
37 determine the, often very complex, adsorption isotherms in order to perform computer assisted
38 optimization to determine the optimal operational conditions [1,6]. “Optimal conditions” often mean
39 maximal production rate and/or minimum solvent consumption but it depends in fact on the
40 particular goal of the separation; e.g. it desirable to have as robust, safe and environmentally friendly
41 processes as possible [7].

42 Adsorption isotherms are often classified according to their shapes [8]. The most common ones is
43 Type-I (Langmuir or similar) that are convex functions with a horizontal asymptote equal to the
44 surface capacity. Type-III adsorption isotherms, sometimes called anti-Langmuir, on the other hand
45 are concave with a vertical asymptote. Type-II, Type-IV, Type-V and Type-VI adsorption isotherms are
46 more complex and contain at least one inflection point. Although there are many cases where the
47 adsorption is best described by complex adsorption isotherms containing inflection points [9–12], for
48 most liquid separation systems the adsorption is best described with Type-I adsorption isotherms
49 that can have one (e.g. Langmuir) or several different adsorption sites (e.g. bi-Langmuir). The
50 Langmuir model has a unimodal energy distribution and the bi-Langmuir has a heterogenic bimodal
51 energy distribution. The bi-Langmuir model has successfully been used to describe the adsorption of
52 enantiomers to protein and cellulose derivatized stationary phases [5], the adsorption of charged

53 solutes [13] and the adsorption of uncharged solutes having both polar and nonpolar properties, e.g.
54 phenol and caffeine [14]. The Tóth adsorption isotherm is an example of a one-site adsorption model
55 that has a unimodal heterogeneous adsorption energy distribution and therefore accounts well for
56 some energetically heterogeneous surfaces, e.g. polar hydrogen bindings between a polar surface
57 and hydrogens at different positions in a peptide [15].

58 There are several chromatographic methods that can be used to measure adsorption isotherms, all
59 with their advantages and drawbacks. Some methods are based on experiments where a constant
60 stream of the solute molecules is introduced in the column, so called plateau methods. Other
61 methods are based on processing of a few overloaded elution profiles. The Frontal Analysis (FA)
62 plateau method is usually carried out in a series of programmed concentration steps, each step
63 resulting in a so called breakthrough front giving one point on the adsorption isotherm curve. In the
64 Perturbation Peak (PP) plateau method, a plateau is established and a small sample, with
65 composition deviating from the plateau, is injected. The disturbance of the established equilibrium
66 generates perturbation peaks with retention times related to the adsorption at that particular
67 plateau level. The FA method is traditionally considered to be the most accurate one for
68 determination of adsorption isotherms and it can be used for any type of adsorption [16]. However,
69 it was recently showed that the PP method is as accurate as the FA method [17]. In both methods it
70 is important to cover a large range of concentration plateau levels which is time-consuming, tedious
71 and consumes large amounts of, often, expensive solutes.

72 The simplest method to obtain adsorption isotherms directly from overloaded elution profiles is
73 Elution by Characteristic Points (ECP) where the diffuse tail of a large overloaded profile is integrated
74 [1]. The ECP method is derived from the ideal model that assumes infinite column efficiency, but
75 since the efficiency of a real column is finite this results in an error in the derived isotherms; the
76 lower the column efficiency the larger the error [18]. Furthermore, the ECP theory assumes
77 rectangular injection profiles which leads to large errors for the large injection volumes that are

78 necessary to obtain sufficient overloading. Due to considerable post-loop dispersion for large
79 injections the injection profiles will have extremely tailed rears. However, it was recently
80 demonstrated, and validated, how easily this this source of error can be eliminated by using the so
81 called ECP-CUT method where a sharp slice is made on the rear of the injection sample zone before
82 introduction into the column [19]. Interesting, and logically, is that the post-loop dispersion is not a
83 problem when using ECP for Type-III adsorption isotherms [2].

84 The most recently developed method for adsorption isotherm determination is the so called Inverse
85 Method (IM) [20–22]. Here adsorption isotherm parameters are determined from a few overloaded
86 elution profiles in a fitting procedure that uses the whole profile, not only the rear as in ECP. The
87 solute consumption and time requirements are very modest compared to plateau methods.
88 However, as opposed to plateau methods, such as FA, adsorption data are not obtained directly from
89 IM. Instead parameters in an adsorption isotherm model are estimated by solving an inverse partial
90 differential equation problem by iteratively simulating elution profiles until the difference is small
91 between the simulated and the experimental elution profiles.

92 To summarize, plateau methods, such as FA and PP, are usually more accurate for adsorption
93 isotherm determination compared to methods based on overloaded elution profiles, such as ECP and
94 IM [1,17]. On the other hand the latter methods are much faster since the whole adsorption
95 isotherm can be obtained from a few overloaded experiments. The ECP method has serious inherent
96 problems and is limited to a few types of adsorption isotherms (mainly Type-I and III) and can only be
97 used for single component adsorption isotherms. IM on the other hand can be used for multi-
98 component problems and for separations with low column efficiency; IM is therefore the primary
99 choice today for preparative and process chromatography. The great advantage with IM is the saving
100 of laboratory time and solvents. One serious disadvantage with IM is that it cannot provide
101 adsorption isotherm data directly; it can only estimate adsorption isotherm parameters in an

102 adsorption isotherm model. This requires that one selects an appropriate adsorption isotherm model
103 prior to estimation.

104 It should be noted that small variations in the adsorption isotherm can be difficult to detect using
105 plateau method as these small variations can be “hidden” between the measured data points and in
106 the general experimental noise. However, extremely small variations, barely visible in the raw
107 adsorption isotherm plot, can have a tremendous impact on the eluted overloaded profile. An
108 interesting example of this is given in [3]. Here the elution profile, see Fig. 9 in [3], has a strange
109 shape where the retention initially increases with increasing sample concentration, but further
110 increases in the sample concentration decreases the retention. Such elution profiles can only be the
111 result of having an inflection point in the corresponding adsorption isotherm. However, this
112 inflection point is barely visible in the adsorption isotherm, see Fig. 4 in [3]. This illustrates how
113 extremely sensitive the elution profiles are to a change in the adsorption isotherm. There are also
114 several examples of complicated adsorption isotherms, with inflection points, that gives very
115 “strange” elution profiles [9].

116 Because of the above, IM, that utilizes the whole elution profiles, could be a much better alternative
117 than the plateau methods to handle very complicated adsorption behavior with, barely visible,
118 (multiple) inflection points in the adsorption isotherm. However, IM is currently restricted by the
119 need to choose an appropriate adsorption isotherm model prior to estimation. One should of course
120 always strive to understand the adsorption behavior of the system and use this understanding to
121 select a proper adsorption isotherm, or to derive a new adsorption isotherm; e.g. see [23] for an
122 example of how a complex adsorption isotherm is derived. However, this might be very hard, or even
123 impossible, for more complicated adsorption behavior. The purpose of this article is to solve the
124 problem in these cases by approximating the adsorption isotherm with monotone piecewise
125 interpolation, in a modified IM, instead of using a closed adsorption isotherm model.

126 The idea of using interpolation instead of a closed adsorption isotherm model has previously been
127 investigated by Haghpanah et al in [24]. They used the Transport Dispersive model with a Linear
128 Driving Force mass transfer model and estimated piecewise linear adsorption isotherms by the
129 Inverse Method (IM) with a Sequential Quadratic Programming algorithm. They successfully applied
130 the method to Type I and III adsorption (no inflection points) and to simple Type II adsorption (one
131 inflection point). Here we will instead use Stineman interpolation [25] that offers significant
132 advantages over the linear interpolation used in [24]. Significantly fewer segments are needed to
133 estimate a nonlinear function with Stineman interpolation than with linear interpolation. In Fig. 1(a)
134 it is shown that only 8 segments are needed to estimate a non-linear adsorption isotherm with
135 Stineman interpolation whereas 24 is needed using linear interpolation to achieve the same
136 accuracy. This means that the numbers of unknown parameters in the inverse problem will be
137 considerably less when using Stineman interpolation compared to linear interpolation. More
138 important is that Stineman interpolation has continuous derivatives whereas linear interpolation has
139 discontinuous ones, see Fig. 1(b). This means that adsorption isotherms estimated using linear
140 interpolation cannot be used by the reliable algorithms for chromatographic calculations that
141 requires continuous adsorption isotherm derivative, such as Orthogonal Collocation On Finite Elements
142 [26] or the Finite Volumes [27,28] algorithm for the Equilibrium-Dispersive model [1] that is used
143 here.

144 When we are dealing with complicated adsorption behavior with multiple inflection points it is of
145 utmost importance the algorithm converge to achieve an acceptable solution and to not get stuck in
146 local minima. For this purpose, we need to use a global optimization algorithm in IM, instead of a
147 local one as used in [24]. Here we will use a derivative free parallelized pattern search optimization
148 algorithm [29]. Notice that because we are dealing with inflection points that are barely visible in the
149 adsorption isotherm we use IM to estimate dq/dC (i.e., the derivative of the stationary phase
150 concentration with respect to the mobile phase concentration) instead of $q(C)$ as in [24].

151 Initially we will study how small very small perturbations in a Type I adsorption isotherm, that
152 generates inflection points, will affect the corresponding overloaded elution profiles. We will then
153 study a specific a synthetic system where the inflection points in the adsorption isotherm are
154 “hidden” and show how the modified IM can successfully estimate an adsorption isotherm in this
155 case. Finally we will test our approach on a real chromatographic separation, with possible inflection
156 points in the adsorption isotherm, and show that the modified IM can successfully be used also in
157 this case. It should be emphasized that the goal here is to use the estimated adsorption isotherms to
158 improve process chromatography and to optimize the purification processes, not necessarily to
159 obtain deeper mechanistic knowledge.

160 **2 Theory**

161 In order to simulate the chromatographic process we need a column model and an adsorption
162 model. As the column model we will use the Equilibrium Dispersive model [1]. Instead of the usual
163 closed expressions, e.g. the Langmuir adsorption model, as adsorption model we will use monotone
164 piecewise interpolation to estimate dq/dC , i.e., the derivative of the stationary phase concentration
165 with respect to the mobile phase concentration. Here we divide the mobile phase concentration
166 range into a finite number of segments and in each segment we will have a monotone function
167 interpolating between the segments boundary points such that continuity, up to a certain order, is
168 preserved across the boundaries. Note that, for example, ordinary cubic splines do not have
169 monotone functions interpolating between segment boundaries (knots) and we will use Stineman
170 interpolation [25], that have continuous derivative, instead.

171 The Inverse Method (IM) of adsorption isotherm estimation is based on adjusting the adsorption
172 isotherm until the difference between experimental elution profiles and elution profiles simulated
173 using the adsorption isotherm is small [22], i.e., we solve the inverse problem. In the usual IM the

174 adsorption isotherm is adjusted by changing the adsorption isotherm parameters in some adsorption
175 model, here we will instead adjust the values of dq/dC at the interpolation segment boundary points.

176 **3 Procedures & Experimental**

177 **3.1 Synthetic System**

178 The synthetic system investigated in section 4.1 - 4.3 was a 250 x 5 mm column with porosity 0.6 and
179 7 000 theoretical plates. The flow rate was 1.0 mL/min and we simulated a single 500 μ L injection
180 with square injection profile and concentration 0.1 g/L.

181 **3.2 Materials and Experimental System**

182 Here the material and chemicals used for the experimental system investigated in section 4.4 is
183 given. The mobile phase was made from HPLC grade methanol (Fisher Scientific, Loughborough, UK)
184 and water from a Milli-Q Plus 185 water purification system (Merck Millipore, Billerica, MA, USA).
185 The buffer in the water part of the mobile was prepared using analytical grade sodium phosphate
186 dibasic dehydrate and sodium phosphate monobasic dihydrate (Sigma-Aldrich, St. Louis, MO, USA).
187 The solute omeprazole sodium monohydrate (> 99%) was from AstraZeneca R&D Mölndal, Sweden,
188 while sodium nitrate (\geq 99.0%) from Sigma-Aldrich was used to determine the column hold-up time.
189 Aqueous buffers and sample solutions were filtered through a 0.2 μ m nylon filter membrane
190 (Whatman, Maidstone, UK) before use. The HPLC instrument was an Agilent 1200 chromatograph
191 system (Agilent Technologies, Palo Alto, CA, USA) equipped with a binary pump, an auto sampler, a
192 diode-array UV-detector and a thermostat-column oven. The stationary phase was an XBridge BEH
193 C₁₈, 100 x 4.6 mm column packed with 3.5 μ m particles (Waters, Milford, MA, USA), with porosity
194 was 0.6157 and number of theoretical plates were 13 895, was operated at 30°C. The mobile phase
195 methanol/phosphate buffer with 35% v/v methanol and pH 8.0 was pumped at a flow rate of 0.7
196 mL/min. Four injections were done, 5 μ L of 0.02 g/L Omeprazole and 300, 400, 500 μ L of 3.53 g/L

197 Omeprazole, and the corresponding injection and elution profiles were measured. The 5 μ L analytical
198 peak was detected at 220 nm while the other overloaded peaks were detected at 342 nm

199 **3.3 Calculations**

200 A finite volume solver with a Koren flux limiter was used to numerically estimate the solution to the
201 Equilibrium-Dispersive model [27,28]. In the Inverse Method (IM) l_1 -norm, i.e., absolute distance was
202 used to measure the difference between experimental and simulated elution profiles and the elution
203 profile areas were normalized so that all experimental elution profiles had the same weight. To solve
204 the inverse problem we used a global, derivative free parallelized pattern search optimization
205 algorithm [29].

206 All calculations were done using MATLAB R2012a on computer cluster consisting of five Intel® Core™
207 i7-3770S 3.10 GHz CPUs with in total 20 calculation cores.

208 **4 Results**

209 In section 4.1 we will begin by studying how a small perturbation to a Type I adsorption isotherm will
210 affect the corresponding overloaded elution profiles. In section 4.2 we will study a specific synthetic
211 chromatographic system and in section 4.3 we will estimate this systems complicated adsorption
212 isotherm by using a modified Inverse Method (IM). Finally, in section 4.4 we will validate our
213 approach for estimation of an adsorption isotherm with inflection points for a real system.

214 **4.1 Impact of Inflection Points**

215 Here we will investigate how the position of very small variations in an adsorption isotherm, that
216 generates inflection points, will influence the shape of the corresponding elution profile. The
217 adsorption isotherm studied in this section will be the Tóth adsorption isotherm,

218

$$q = q_s \frac{C}{(1/K + C^\nu)^{1/\nu}}, \quad (1)$$

$$\frac{dq}{dC} = q_s \frac{1}{(1 + \nu K C^{\nu-1})(1/K + C^\nu)^{1/\nu}},$$

219 where $q_s = 2.563$, $K = 1.369$ and $\nu = 0.882$. Now let's modify the adsorption isotherm in Eq. (1) by
 220 adding a very small, normal distributed, perturbation according to,

221

$$\tilde{q} = q_s \frac{C}{(1/K + C^\nu)^{1/\nu}} + \frac{a}{\sigma \sqrt{2\pi}} \left(e^{-\frac{(C-C_0)^2}{2\sigma^2}} - e^{-\frac{C_0^2}{2\sigma^2}} \right), \quad (2)$$

$$\frac{d\tilde{q}}{dC} = q_s \frac{1}{(1 + \nu K C^{\nu-1})(1/K + C^\nu)^{1/\nu}} - \frac{a(C - C_0)}{\sigma^3 \sqrt{2\pi}} e^{-\frac{(C-C_0)^2}{2\sigma^2}},$$

222 where C_0 is the location of the perturbation in the adsorption isotherm, $a = 10^{-5}$ is the amplitude of
 223 the perturbation and $\sigma = 2 \cdot 10^{-3}$ is the width of the perturbation. In Fig. 2 (a) the Tóth adsorption
 224 isotherm in Eq. (1) is shown together with the modified Tóth adsorption isotherm in Eq. (2) at
 225 location $C_0 = 0.012$ g/L. In the insert the corresponding derivative is shown. Notice that the very small
 226 perturbation is almost invisible in the adsorption isotherm, but the difference in the corresponding
 227 derivative is clearly visible and we see that the perturbation introduces several inflection points. The
 228 corresponding elution profiles for a 500 μ L injection of 0.1 g/L sample are shown in Fig. 2 (b). As can
 229 be seen the very small perturbation in the Type I adsorption isotherm has a very large effect on the
 230 shape of the corresponding elution profile.

231 Now we want to see how the location in the adsorption isotherm of the perturbation generating the
 232 inflection point, i.e., C_0 in Eq. (2) above, will affect the difference in elution profiles. We will study the
 233 same injection as in Fig. 2, i.e., a 500 μ L injection of 0.1 g/L sample, and use the l_1 -norm of the
 234 residual vector to measure the difference between the elution profiles. The result is shown in Fig. 3
 235 and as can be seen a perturbation in the adsorption isotherm will have larger effect the earlier it
 236 appears. The effect of the perturbation on the shape of the elution profile initially decreases very

237 rapidly, thereafter the decrease in effect is more modest until the maximum eluted concentration
238 where the effect again decreases very rapidly up to the injected concentration. After the injected
239 concentration, the perturbation has almost no effect on the elution profile (notice that the highest
240 concentration inside the column might be higher than the injected concentration).

241 4.2 Example Chromatographic System

242 Assume that we have measured 20 data points on the adsorption isotherm for the system (see
243 section 3.1 for system details), e.g. by using frontal analysis. These data points are shown as symbols
244 in Fig. 4 (a). From the data points and the Scatchard plot in the inset it is “obvious” that we have
245 heterogeneous Type I (Langmuir Type) adsorption and therefore a heterogeneous Type I adsorption
246 isotherm model should be used. Here we fitted the Tóth adsorption model in Eq. (1), with three
247 parameters, q_s , K , ν , to the data points and got that $q_s \approx 2.563$, $K \approx 1.369$ and $\nu \approx 0.882$ (the same
248 values used in section 4.1). As can be seen in Fig. 4 (a) the fit is excellent.

249 In Fig. 4 (b) the measured elution profile is shown together with an elution profile simulated using
250 the estimated Tóth adsorption isotherm above. As can be seen the shape of the experimental profile
251 looks strange and the tail of the elution profiles doesn't match at all. This might lead to the
252 conclusion that there is something wrong with the experiments, e.g. that the injected sample
253 contains impurities.

254 Now let us take a closer look at the true adsorption isotherm that is shown together with the
255 estimated Tóth isotherm in Fig. 5. In Fig. 5 (a) there is a very slight difference in the initial part of the
256 adsorption isotherms but this difference falls between the measured data points and is therefore not
257 detected in the experiments. In Fig. 5 (b) the derivative dq/dC of the adsorption isotherms are shown
258 and as can be seen the small deviation not only gives rise to large difference in the derivative of the
259 adsorption isotherm but also to two inflection points, i.e., extreme points in the derivative. This is
260 what actually causes the large difference in the overloaded elution profiles seen in Fig. 4 (b).

261 4.3 Modified Inverse Method

262 As the effect of the slight deviation in the true adsorption is clearly visible in the overloaded elution
 263 profile in Fig. 4 (b) the Inverse Method (IM) should be able to estimate the true adsorption isotherm.
 264 However in Fig. 5 (b) we see that we have two inflection points and if we are going to use IM we
 265 need to select an adsorption isotherm model with two inflection points. One option is the bi-Moreau
 266 model,

$$267 \quad q = q_{s,1} \frac{K_1 C + h_1 K_1^2 C^2}{1 + 2K_1 C + h_1 K_1^2 C^2} + q_{s,2} \frac{K_2 C + h_2 K_2^2 C^2}{1 + 2K_2 C + h_2 K_2^2 C^2}, \quad (3)$$

268 with six parameters $q_{s,*}$, h_* , K_* . As the inflection points are more clearly visible in the derivative of the
 269 adsorption isotherm, see Fig. 5 (b), it is better to try to estimate the derivative of the adsorption
 270 isotherm by IM. For the bi-Moreau adsorption isotherm we have that,

$$271 \quad \frac{dq}{dC} = K_1 q_{s,1} \frac{1 + 2h_1 K_1 C + h_1 K_1^2 C^2}{(1 + 2K_1 C + h_1 K_1^2 C^2)^2} + K_2 q_{s,2} \frac{1 + 2h_2 K_2 C + h_2 K_2^2 C^2}{(1 + 2K_2 C + h_2 K_2^2 C^2)^2}. \quad (4)$$

272 If we estimate $q' = dq/dC$ the corresponding adsorption isotherm q is of course,

$$273 \quad q(C_0) = \int_{C=0}^{C_0} q'(C) dC. \quad (5)$$

274 In order to check if the bi-Moreau adsorption isotherm is a viable choice for the IM in this case, we
 275 begin by checking if we can fit dq/dC in Eq. (4) to the derivative of the actual adsorption isotherm in
 276 Fig. 5 (b), at least up to the highest eluted concentration. The fitting was done by using several runs
 277 with a global genetic algorithm [30] combined with a Levenberg-Marquardt local least squares solver
 278 [31]; the best fit achieved is shown in Fig. 6. As can be seen from the figure the bi-Moreau adsorption
 279 isotherm can most likely not be used to model the adsorption in this case. This means that it is very
 280 hard, and can even be impossible, to find an adsorption isotherm model that can be used here.

281 Because of the above we will instead try to estimate a monotone piecewise interpolation
282 approximation to the adsorption isotherm by IM rather than using an adsorption isotherm model of
283 any kind, i.e., we do not assume any adsorption isotherm model, see Theory section. The only
284 starting user input needed is to select the number of interpolation points and where they should be
285 placed on the mobile phase concentration axis of the adsorption isotherm. Thereafter, the
286 corresponding stationary phase concentration at these points, and the interpolation between them,
287 is estimated by the optimization procedure. There is no exact rule giving the number of interpolation
288 points needed. If the number of interpolations are too few one will not be able to accurately
289 estimate a piece-wise approximation to the actual adsorption isotherm and hence will not be able to
290 get a good fit to the elution profiles. On the other hand, if the number of interpolation points are too
291 more than required, the optimization procedure will take very long time. From our experience in this
292 study, as a rule of thumb ~ 10 interpolation points is usually sufficient for Langmuir or anti-Langmuir
293 shaped elution profiles whereas for more unusual and strange elution profiles around 20 – 30 points
294 should be used. Note that one can easily add more interpolation points to an obtained solution and
295 rerun to refine the solution if the fit to the experimental elution profiles is not satisfactory. In this
296 case we will use 20 interpolation points (19 segments). As we saw in section 4.1 the initial part of the
297 adsorption isotherm is more important and we will therefore use an uneven distribution of the
298 interpolation points, i.e., uneven length of the segments. Up to 20% of the maximum eluted
299 concentration we will place 8 equally spaced interpolation points, from 20% up to 100% of the
300 maximum eluted concentration we will place 8 equally spaced interpolation points and from 100% of
301 the maximum eluted concentration up to two times the sample concentration we will place 4 equally
302 spaced interpolation points.

303 It should be noted that estimation of monotone piecewise interpolation approximation to an
304 adsorption isotherm is a considerably harder and more costly inverse problem than estimation of
305 parameters in an adsorption isotherm function. To solve this problem we will use a parallelized
306 global pattern search algorithm on a computer cluster with 20 calculation cores and as starting guess

307 we will use discretization of the Tóth adsorption isotherm in Fig. 5. The estimated discretized
308 adsorption isotherm is shown in Fig. 7 (a-b). In the figures there are clear differences between
309 estimates and the true adsorption isotherm, note especially that we have very large difference above
310 the maximum eluted concentration. However, this part of the adsorption isotherm has almost no
311 effect on the position and shape of the elution profile, see section 4.1. In Fig. 7 (c) the experimental
312 elution profile is shown together with an elution profile simulated using the discretized adsorption
313 isotherm, as can be seen the fit shows now excellent agreement with the experimental data.

314 **4.4 Real Systems**

315 We tested our approach on a chromatographic HPLC system consisting of an XBridge BEH C10
316 column with methanol/phosphate buffer (35%/65% v/v, pH 8.0) as mobile phase, section 3.2 for
317 more experimental details. Different injection of Omeprazole was done; in Fig. 8 (a) the elution
318 profiles for overloaded 300 and 400 μL (main figure) and an analytical 5 μL injection (inset) are
319 shown. Notice the extremely shallow and quite long plateau at the end of the large volume profiles
320 The experimental overloaded profiles has indeed strange shapes and for this reason here serves as a
321 challenging real system case. This plateau might have several reasons, e.g. degradation of the sample
322 or impurities, or pH-instability, and warrants further investigation. Regardless of the reason such
323 profiles are not impossible; even stranger profiles have been reported in the literature and some of
324 them can also be explained [32,33].

325 Here the strange profiles will serve as a challenging case example and we will show that the plateau
326 *might* also be the result of inflection points in the adsorption isotherm. Here we used the elution
327 profiles from four injections in the modified IM to estimate a discretized adsorption isotherm with 30
328 interpolation points (29 segments). As in section 4.3 we will use an uneven distribution of the
329 interpolation points: Up to 20% of the maximum eluted concentration we will place 12 equally
330 spaced interpolation points, from 20% up to 100% of the maximum eluted concentration we will
331 place 12 equally spaced interpolation points and from 100% of the maximum eluted concentration

332 up to two times the sample concentration we will place 6 equally spaced interpolation points. Please
333 note that we does not use an adsorption isotherm model of any kind, i.e., we do not assume any
334 adsorption isotherm model, see Theory section. The results presented in Fig. 8 (a) shows an excellent
335 agreement was achieved between the experimental and the calculated profiles and we were able to
336 estimate an adsorption isotherm that accounted well for the small plateau at the end. The estimated
337 discretize adsorption isotherm is shown in Fig. 8 (b), please notice the inflection points in the inset.

338 **5 Conclusions**

339 We have shown that even very small variation in the adsorption isotherm might give rise to inflection
340 points in the adsorption isotherm that have a tremendous impact on the shape of the elution
341 profiles, see Fig. 3. The earlier in the adsorption isotherm these variations occur the larger the
342 impact, but the impact decreases rapidly with increasing adsorption isotherm mobile phase
343 concentration. We have also shown that inflection points might be missed when using traditional
344 experimental plateau methods for adsorption isotherm determination, such as Frontal Analysis (FA).
345 Here it should be noted that these traditional methods also have less accuracy at the lower
346 concentration regions of the isotherm [17]. Furthermore we have shown that it might not be possible
347 to find a closed adsorption isotherm model that account for these inflection points. We have
348 therefore developed and validated a modified Inverse Method (IM), which uses monotone piecewise
349 interpolation instead of a fixed adsorption isotherm model, to solve the problem of estimating
350 adsorption isotherms where small variations give rise to inflection points. We demonstrated, both for
351 a synthetic and a real case, that the method was able to successfully estimate adsorption isotherm
352 with multiple inflection points.

353 Plateau methods, such as FA, measures points on the adsorption isotherm curve and the modified IM
354 can be viewed as a way to indirectly estimate points on the adsorption isotherm curve (or the
355 derivative of it) from overloaded elution profiles. Here we have studied single component cases, but

356 the principle of using IM with interpolation could, in principle, be extended to also two component
357 cases. However, in this case we need to estimate an interpolated competitive adsorption isotherm
358 surface which is a considerably harder problem.

359 It should be noted that it is not possible to draw conclusions about the adsorption mechanism from
360 monotone piecewise interpolation approximations in the same way as it is for the parameters in a
361 closed adsorption isotherm model. However, if the goal is to optimize the purification process piece-
362 wise approximation is sufficient. Moreover, the piece-wise approximation can also be used as a
363 starting point to derive a closed expression for the adsorption isotherm, e.g., the putative closed
364 expression can be fitted to the piece-wise approximation and one can then both judge if the closed
365 expression is a good option and, if it is, get the adsorption isotherm parameters in the closed
366 expression.

367 It should also be noted that estimation of monotone piecewise interpolation approximations is a
368 considerably harder and more costly inverse problem than determination of parameters in a closed
369 adsorption isotherm model using IM. Therefore the modified IM should only be used as an option for
370 estimation of complicated adsorption isotherms in cases where nothing else works.

371 **Acknowledgement**

372 This work was supported by the Swedish Research Council (VR) in the project "*Fundamental studies*
373 *on molecular interactions aimed at preparative separations and biospecific measurements*" (grant
374 number 621-2012-3978), by the Swedish Knowledge Foundation for the KK HÖG 2014 project "*SOMI:*
375 *Studies of Molecular Interactions for Quality Assurance, Bio-Specific Measurement & Reliable*
376 *Supercritical Purification*" (grant number 20140179) and by the INTERACT research environment at
377 Karlstad University.

378 **References**

- 379 [1] G. Guiochon, D.G. Shirazi, A. Felinger, A.M. Katti, *Fundamentals of preparative and nonlinear*
380 *chromatography*, 2nd ed., Academic Press, Boston, MA, 2006.
- 381 [2] J. Samuelsson, T. Undin, T. Fornstedt, Expanding the elution by characteristic point method for
382 determination of various types of adsorption isotherms, *J. Chromatogr. A.* 1218 (2011) 3737–
383 3742. doi:10.1016/j.chroma.2011.04.035.
- 384 [3] A. Seidel-Morgenstern, G. Guiochon, Modelling of the competitive isotherms and the
385 chromatographic separation of two enantiomers, *Chem. Eng. Sci.* 48 (1993) 2787–2797.
386 doi:10.1016/0009-2509(93)80189-W.
- 387 [4] T. Fornstedt, Characterization of adsorption processes in analytical liquid–solid chromatography,
388 *J. Chromatogr. A.* 1217 (2010) 792–812. doi:10.1016/j.chroma.2009.12.044.
- 389 [5] J. Samuelsson, R. Arnell, T. Fornstedt, Potential of adsorption isotherm measurements for closer
390 elucidating of binding in chiral liquid chromatographic phase systems, *J. Sep. Sci.* 32 (2009)
391 1491–1506. doi:10.1002/jssc.200900165.
- 392 [6] P. Forssén, J. Samuelsson, T. Fornstedt, Relative importance of column and adsorption
393 parameters on the productivity in preparative liquid chromatography. I: Investigation of a chiral
394 separation system, *J. Chromatogr. A.* 1299 (2013) 58–63. doi:10.1016/j.chroma.2013.05.031.
- 395 [7] J. Samuelsson, M. Enmark, P. Forssén, T. Fornstedt, Highlighting Important Parameters Often
396 Neglected in Numerical Optimization of Preparative Chromatography, *Chem. Eng. Technol.* 35
397 (2012) 149–156. doi:10.1002/ceat.201100210.
- 398 [8] K.S.W. Sing, D.H. Everett, R.A.W. Haul, L. Moscou, R.A. Pierotti, J. Rouquerol, et al., Reporting
399 physisorption data for gas/solid systems with special reference to the determination of surface
400 area and porosity, *Pure Appl. Chem.* 57 (1985) 603–619. doi:10.1351/pac198557040603.

- 401 [9] W. Zhang, Y. Shan, A. Seidel-Morgenstern, Breakthrough curves and elution profiles of single
402 solutes in case of adsorption isotherms with two inflection points, *J. Chromatogr. A.* 1107 (2006)
403 216–225. doi:10.1016/j.chroma.2005.12.094.
- 404 [10] F. Gritti, G. Guiochon, Adsorption mechanism of acids and bases in reversed-phase liquid
405 chromatography in weak buffered mobile phases designed for liquid chromatography/mass
406 spectrometry, *J. Chromatogr. A.* 1216 (2009) 1776–1788. doi:10.1016/j.chroma.2008.10.064.
- 407 [11] F. Gritti, G. Guiochon, Peak shapes of acids and bases under overloaded conditions in reversed-
408 phase liquid chromatography, with weakly buffered mobile phases of various pH: A
409 thermodynamic interpretation, *J. Chromatogr. A.* 1216 (2009) 63–78.
410 doi:10.1016/j.chroma.2008.11.020.
- 411 [12] M. Enmark, J. Samuelsson, T. Undin, T. Fornstedt, Characterization of an unusual adsorption
412 behavior of racemic methyl-mandelate on a tris-(3,5-dimethylphenyl) carbamoyl cellulose chiral
413 stationary phase, *J. Chromatogr. A.* 1218 (2011) 6688–6696. doi:10.1016/j.chroma.2011.07.064.
- 414 [13] T. Undin, J. Samuelsson, A. Törnåcrona, T. Fornstedt, Evaluation of a combined linear–nonlinear
415 approach for column characterization using modern alkaline-stable columns as model, *J. Sep. Sci.*
416 36 (2013) 1753–1761. doi:10.1002/jssc.201201132.
- 417 [14] F. Gritti, G. Guiochon, Role of the buffer in retention and adsorption mechanism of ionic species
418 in reversed-phase liquid chromatography, *J. Chromatogr. A.* 1038 (2004) 53–66.
419 doi:10.1016/j.chroma.2004.03.036.
- 420 [15] X. Zhang, J. Samuelsson, J.-C. Janson, C. Wang, Z. Su, M. Gu, et al., Investigation of the adsorption
421 behavior of glycine peptides on 12% cross-linked agarose gel media, *J. Chromatogr. A.* 1217
422 (2010) 1916–1925. doi:10.1016/j.chroma.2010.01.058.
- 423 [16] A. Seidel-Morgenstern, Experimental determination of single solute and competitive adsorption
424 isotherms, *J. Chromatogr. A.* 1037 (2004) 255–272. doi:10.1016/j.chroma.2003.11.108.

- 425 [17] J. Lindholm, P. Forssén, T. Fornstedt, Validation of the accuracy of the perturbation peak method
426 for determination of single and binary adsorption isotherm parameters in LC, *Anal. Chem.* 76
427 (2004) 4856–4865. doi:10.1021/ac0497407.
- 428 [18] L. Ravald, T. Fornstedt, Theoretical study of the accuracy of the elution by characteristic points
429 method for bi-Langmuir isotherms, *J. Chromatogr. A.* 908 (2001) 111–130. doi:10.1016/S0021-
430 9673(00)00965-1.
- 431 [19] J. Samuelsson, T. Fornstedt, Injection Technique for Generating Accurate Adsorption Isotherm
432 Data Using the Elution by Characteristic Points Method, *Anal. Chem.* 80 (2008) 7887–7893.
433 doi:10.1021/ac8010999.
- 434 [20] A. Felinger, A. Cavazzini, G. Guiochon, Numerical determination of the competitive isotherm of
435 enantiomers, *J. Chromatogr. A.* 986 (2003) 207–225. doi:10.1016/S0021-9673(02)01919-2.
- 436 [21] A. Felinger, D. Zhou, G. Guiochon, Determination of the single component and competitive
437 adsorption isotherms of the 1-indanol enantiomers by the inverse method, *J. Chromatogr. A.*
438 1005 (2003) 35–49. doi:10.1016/S0021-9673(03)00889-6.
- 439 [22] P. Forssén, R. Arnell, T. Fornstedt, An improved algorithm for solving inverse problems in liquid
440 chromatography, *Comput. Chem. Eng.* 30 (2006) 1381–1391.
441 doi:10.1016/j.compchemeng.2006.03.004.
- 442 [23] F. Gritti, G. Guiochon, Characteristics of the adsorption mechanism of acido-basic compounds
443 with two p in reversed-phase liquid chromatography, *J. Chromatogr. A.* 1216 (2009) 6917–6930.
444 doi:10.1016/j.chroma.2009.07.064.
- 445 [24] R. Haghpanah, A. Rajendran, S. Farooq, I.A. Karimi, M. Amanullah, Discrete Equilibrium Data from
446 Dynamic Column Breakthrough Experiments, *Ind. Eng. Chem. Res.* 51 (2012) 14834–14844.
447 doi:10.1021/ie3015457.
- 448 [25] R.W. Stineman, A Consistently Well-Behaved Method of Interpolation, *Creat. Comput.* 6 (1980)
449 54–57.

- 450 [26] K. Kaczmarski, M. Mazzotti, G. Storti, M. Mobidelli, Modeling fixed-bed adsorption columns
451 through orthogonal collocations on moving finite elements, *Comput Chem Eng.* 21 (1997) 641–
452 660. doi:10.1016/S0098-1354(96)00300-6.
- 453 [27] S. Javeed, S. Qamar, A. Seidel-Morgenstern, G. Warnecke, Efficient and accurate numerical
454 simulation of nonlinear chromatographic processes, *Comput. Chem. Eng.* 35 (2011) 2294–2305.
455 doi:10.1016/j.compchemeng.2010.10.002.
- 456 [28] R.J. LeVeque, *Finite volume methods for hyperbolic problems*, Cambridge University Press,
457 Cambridge ; New York, 2002.
- 458 [29] C. Audet, J.E. Dennis, Analysis of Generalized Pattern Searches, *SIAM J. Optim.* 13 (2002) 889–
459 903. doi:10.1137/S1052623400378742.
- 460 [30] D. Whitley, A genetic algorithm tutorial, *Stat. Comput.* 4 (1994). doi:10.1007/BF00175354.
- 461 [31] T.F. Coleman, Y. Li, An Interior Trust Region Approach for Nonlinear Minimization Subject to
462 Bounds, *SIAM J. Optim.* 6 (1996) 418–445. doi:10.1137/0806023.
- 463 [32] S. Golshan-Shirazi, G. Guiochon, Experimental study of system peaks and elution profiles for
464 large concentration bands in the case of a binary eluent containing a strongly sorbed additive, *J.*
465 *Chromatogr. A.* 461 (1989) 19–34. doi:10.1016/S0021-9673(00)94272-9.
- 466 [33] R. Arnell, P. Forssén, T. Fornstedt, Tuneable peak deformations in chiral liquid chromatography,
467 *Anal. Chem.* 79 (2007) 5838–5847. doi:10.1021/ac062330t.
- 468

469 **Figure Captions (ONLINE)**

470 **Figure 1:** Linear (red curve and circle symbols) vs. Stineman (blue curve and square symbols)
471 interpolation: in (a) interpolation of an adsorption isotherm (solid curve) and in (b) the corresponding
472 derivatives.

473 **Figure 2:** In (a) a Tóth adsorption isotherm (red curve), see Eq. (1), and the same adsorption isotherm
474 modified with a small perturbation (blue curve) at the location indicated by the vertical line, see Eq.
475 (2); in then inset the derivative of the curves is shown. In (b) elution profiles simulated using the
476 adsorption isotherms in (a).

477 **Figure 3:** How the difference between elution profiles, simulated using the Tóth and the modified
478 Tóth adsorption isotherm, varies with the location of the perturbation in modified Tóth adsorption
479 isotherm, see Eq. (1) and Eq. (2). The vertical dotted line indicates the injected concentration and the
480 vertical dashed line indicates maximum eluted concentration in the Tóth adsorption isotherm
481 simulation.

482 **Figure 4:** In (a) measured adsorption isotherm data points (symbols) and a fitted Tóth adsorption
483 isotherm (red curve); in the inset the corresponding Scatchard (q/C) plot is shown. In (b)
484 Experimental (black curve) and simulated (red curve) overloaded elution profiles.

485 **Figure 5:** In (a) measured adsorption isotherm data points (symbols) together with true (blue curve)
486 and fitted Tóth (red curve) adsorption isotherms. A zoomed in view of the initial part in the box is
487 shown in the inset. In (b) derivate of true (blue curve) and fitted Tóth (red curve) adsorption
488 isotherm, the symbols indicate inflection points and the max eluted concentration for the elution
489 profile in Fig. 4 (b) is shown as a vertical dashed line.

490 **Figure 6:** True (blue curve) and fitted bi-Moreau (red curve), see Eq. (3) and Eq. (4), adsorption
491 isotherm.

492 **Figure 7:** Estimated (red curve and symbols) and true (blue curve) adsorption isotherm. In (a) the
493 derivative of the adsorption isotherms up to the highest eluted concentration and in (b) the
494 corresponding adsorption isotherm up to 0.014 g/ L, cf. inset in Fig. 5 (a). The insets in (a) and (b)
495 shows the derivative of the adsorption isotherms and the adsorption isotherm, respectively, up to 2
496 times the injected concentration. In (c) experimental (black curve) and simulated (red curve)
497 overloaded elution profiles.

498 **Figure 8:** In (a) experimental (black curves) and simulated (red curves) elution profiles for 5 (inset),
499 300 and 400 μ L injections of Omeprazole. In (b) the estimated discrete adsorption isotherm (red
500 curve), the line is a diagonal that makes it easier to see deviation from linearity. A zoomed in view of
501 the initial part in the box is shown in the inset. See Section 3.2 for more experimental details.

502 **Figure Captions (PRINT)**

503 **Figure 1:** Linear (dotted curve and circle symbols) vs. Stineman (dashed curve and square symbols)
504 interpolation: in (a) interpolation of an adsorption isotherm (solid curve) and in (b) the corresponding
505 derivatives.

506 **Figure 2:** In (a) a Tóth adsorption isotherm (dotted curve), see Eq. (1), and the same adsorption
507 isotherm modified with a small perturbation (dashed curve) at the location indicated by the vertical
508 line, see Eq. (2); in then inset the derivative of the curves is shown. In (b) elution profiles simulated
509 using the adsorption isotherms in (a).

510 **Figure 3:** How the difference between elution profiles, simulated using the Tóth and the modified
511 Tóth adsorption isotherm, varies with the location of the perturbation in modified Tóth adsorption
512 isotherm, see Eq. (1) and Eq. (2). The vertical dotted line indicates the injected concentration and the
513 vertical dashed line indicates maximum eluted concentration in the Tóth adsorption isotherm
514 simulation.

515 **Figure 4:** In (a) measured adsorption isotherm data points (symbols) and a fitted Tóth adsorption
516 isotherm (dotted curve); in the inset the corresponding Scatchard (q/C) plot is shown. In (b)
517 Experimental (solid curve) and simulated (dotted curve) overloaded elution profiles.

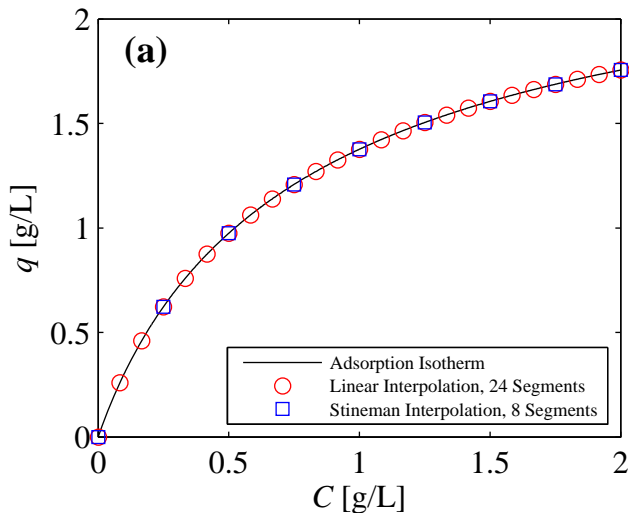
518 **Figure 5:** In (a) measured adsorption isotherm data points (symbols) together with true (dashed
519 curve) and fitted Tóth (dotted curve) adsorption isotherms. A zoomed in view of the initial part in the
520 box is shown in the inset. In (b) derivate of true (dashed curve) and fitted Tóth (dotted curve)
521 adsorption isotherm, the symbols indicate inflection points and the max eluted concentration for the
522 elution profile in Fig. 4 (b) is shown as a vertical line.

523 **Figure 6:** True (dashed curve) and fitted bi-Moreau (dotted curve), see Eq. (3) and Eq. (4), adsorption
524 isotherm.

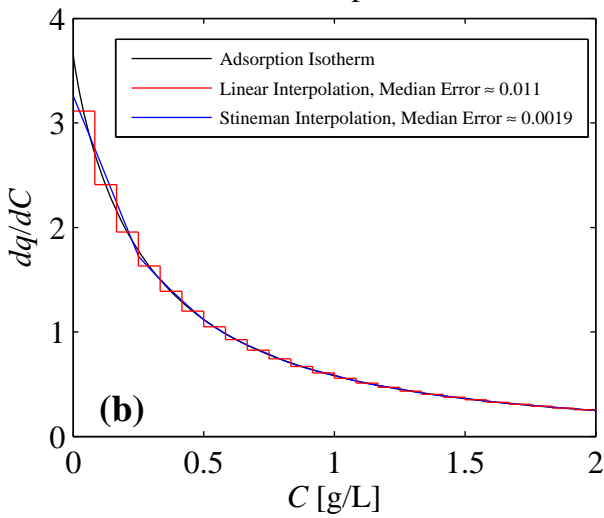
525 **Figure 7:** Estimated (dotted curve and symbols) and true (dashed curve) adsorption isotherm. In (a)
526 the derivative of the adsorption isotherms up to the highest eluted concentration and in (b) the
527 corresponding adsorption isotherm up to 0.014 g/ L, cf. inset in Fig. 5 (a). The insets in (a) and (b)
528 shows the derivative of the adsorption isotherms and the adsorption isotherm, respectively, up to 2
529 times the injected concentration. In (c) experimental (solid curve) and simulated (dotted curve)
530 overloaded elution profiles.

531 **Figure 8:** In (a) experimental (solid curves) and simulated (dotted curves) elution profiles for 5 (inset),
532 300 and 400 μ L injections of Omeprazole. In (b) the estimated discrete adsorption isotherm (dotted
533 curve), the line is a diagonal that makes it easier to see deviation from linearity. A zoomed in view of
534 the initial part in the box is shown in the inset. See Section 3.2 for more experimental details.

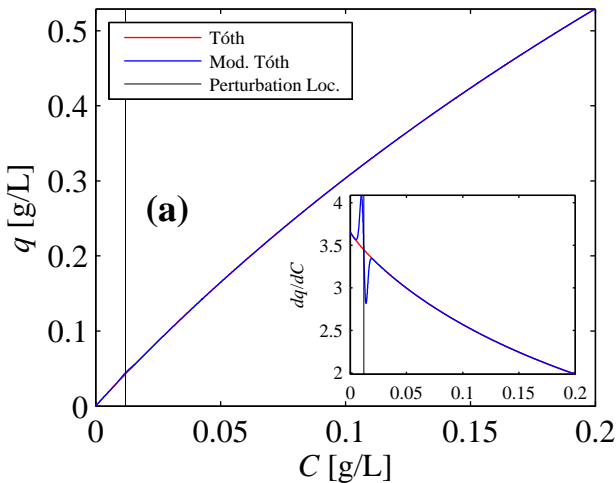
Interpolation, Max Error ≤ 0.01 g/L



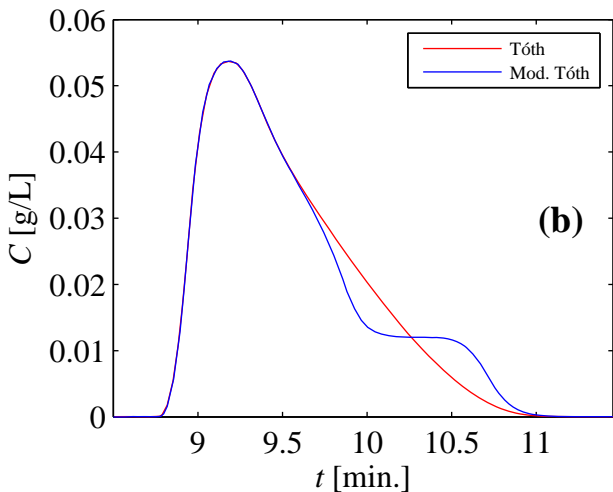
Derivate of Adsorption Isotherms



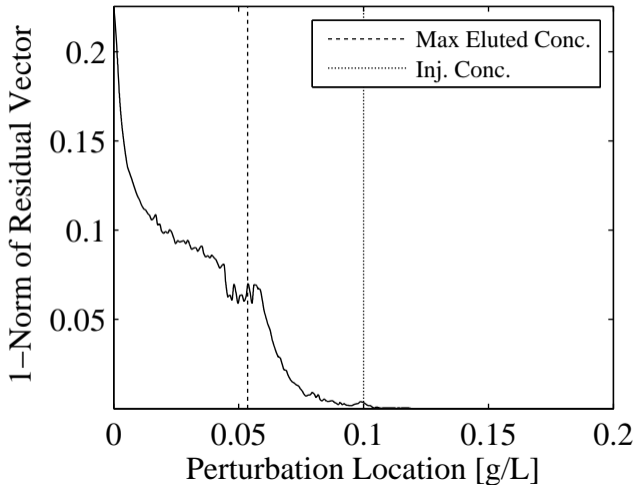
Tóth Adsorption Isotherm



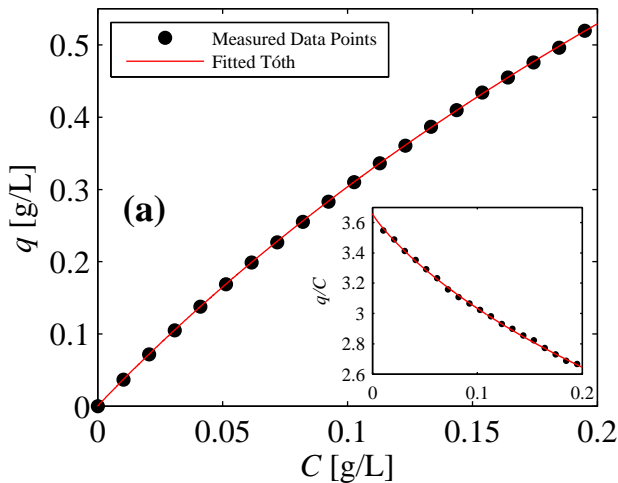
Simulation



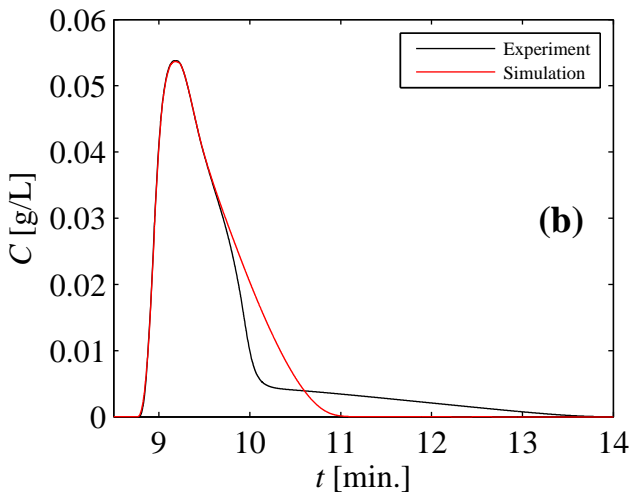
Elution Profile Difference



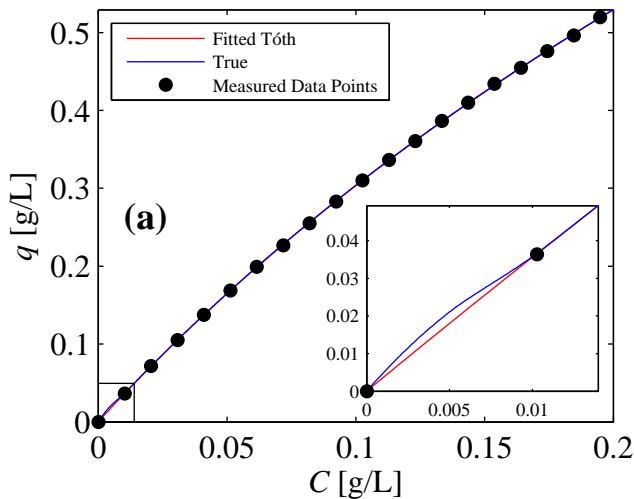
Fitted Tóth Adsorption Isotherm



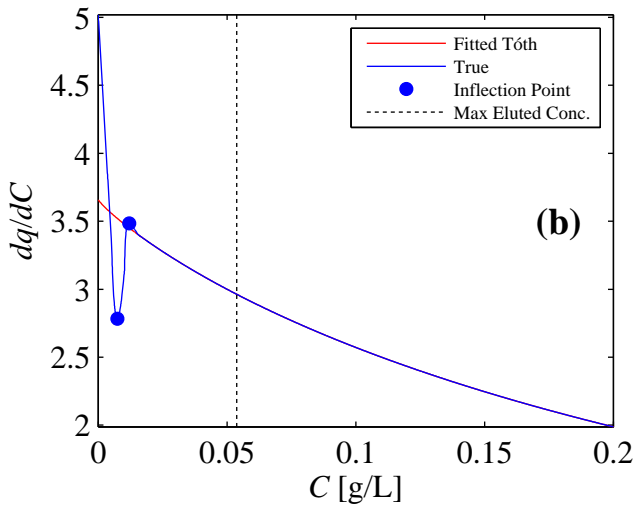
Simulation



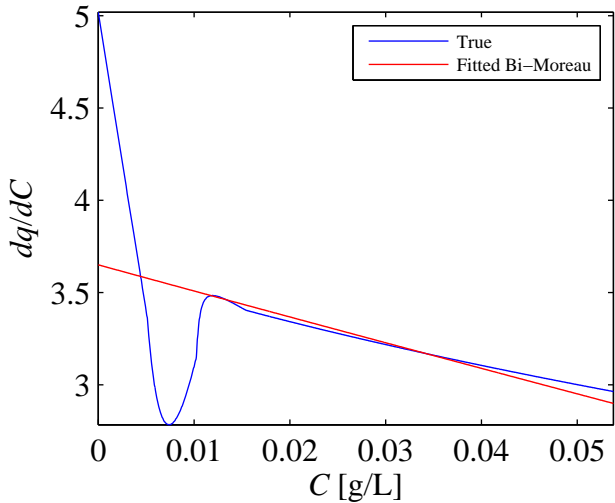
Adsorption Isotherm



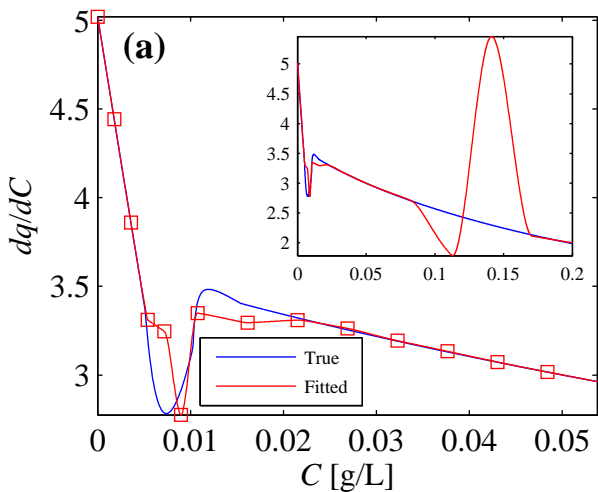
Derivative of Adsorption Isotherm



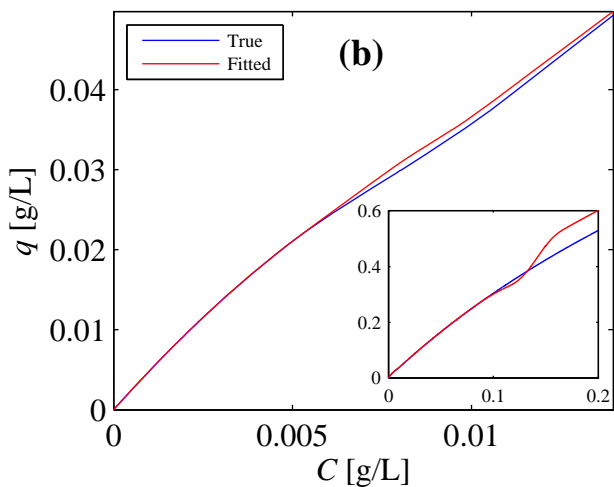
Fitted Bi-Moreau Adsorption Isotherm



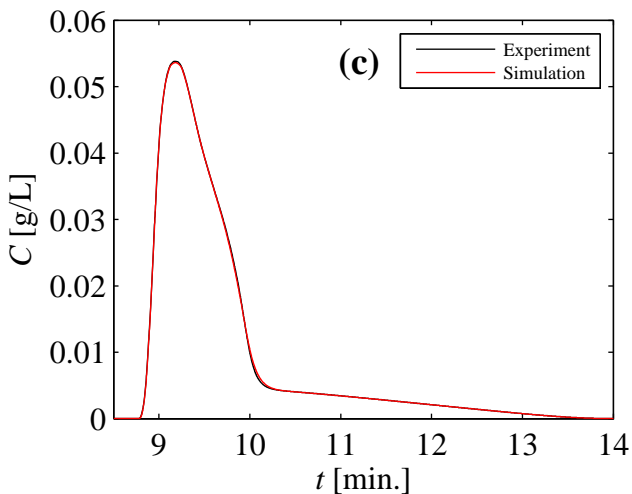
Derivative of Adsorption Isotherms



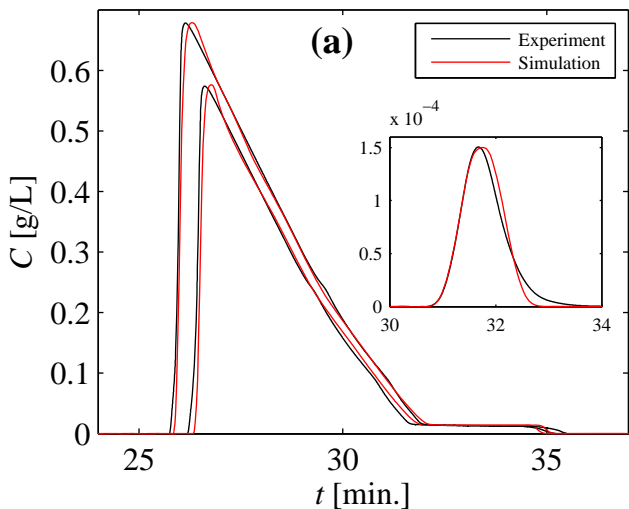
Adsorption Isotherms



Simulation



Elution Profiles



Adsorption Isotherm

